

Sodium Chains as Core Nanowires for Gelation of Organic Solvents from a Functionalized Nicotinic Acid and Its Sodium Salt

David Bardelang,^{*,[a]} Franck Camerel,^[b] Anna C. G. Hotze,^[a] Benson Kariuki,^[a] Biswajit Paik,^[c] Marc Schmutz,^[d] Raymond Ziessel,^{*,[b]} and Michael J. Hannon^{*,[a]}

Abstract: A new metallo-organic gelator formed from an admixture of a substituted nicotinic acid and its sodium salt is described. The nicotinic acid is substituted in the 6-position by an acetal functionality. The crystal structure of the 1:1 mixture revealed that the sodium atoms are aligned in infinite chains with the two organic units hydrogen bonded together to create potentially trinucleating ligands that encase the metal core, which leads to tube-like structures. These one-dimen-

sional crystals were found to spontaneously gelify dichloromethane and provide pyridine gels with high thermal resistance. Gel formation was investigated by several analytical techniques, which included differential scanning calorimetry, TEM, freeze fracture electron microscopy (FFEM), IR spectroscopy

and X-ray diffraction, and was found to be induced by the swelling of the one-dimensional material. FFEM and powder X-ray diffraction have revealed that the sodium chains are associated in a highly compacted state into a layered structure inside the gel. Doping these robust gels with dyes by diffusion, such as xylene cyanol, methyl yellow and bromo thymol blue, is feasible without destruction of the gels.

Keywords: nicotinic acid • organogelators • self-assembly • sodium salts • supramolecular chemistry

Introduction

Gels based on low molecular weight gelators have attracted much attention over the last decade,^[1] primarily owing to emerging functions based on properties that are tuneable by external stimuli, such as light,^[2] temperature,^[1] ultrasound^[3] and chemical additives.^[4] This novel kind of matter has the potential to pave the way for exotic applications for gels, such as confined reaction media,^[5] templates for well-defined inorganic materials^[6] or polymers,^[7] light-harvesting systems,^[8] sensors,^[9] biomaterials^[10] and optoelectronic devices.^[11] The gelation phenomenon is generally described as a series of successive supramolecular events that give rise to three-dimensional architectures, which often consist of fibrillar networks^[12] that entrap solvent molecules in large pockets.^[13] Despite some attempts to predict the gelation capacity of new agents based on families of known gelator structures,^[14] the discovery of new chemical structures with the ability to gel solvents remains largely serendipitous. Several gelation motifs (structures that impart gelation behaviour when grafted onto other compounds) have been reported in the literature. Organic motifs that are known to induce gelation are mainly based on steroids,^[15] peptides,^[16] ureas,^[17] sugars,^[10d,14c-d,18] dendrimers,^[10e,19] porphyrins^[20] and gemini surfactants.^[21] Metallo-organic gelators^[22] have also recently

[a] Dr. D. Bardelang, Dr. A. C. G. Hotze, Dr. B. Kariuki, Prof. M. J. Hannon
School of Chemistry, University of Birmingham
Edgbaston, Birmingham B15 2TT (UK)
Fax: (+44)121-414-4403
E-mail: david.bardelang@nrc.cnrc.gc.ca
m.j.hannon@bham.ac.uk

[b] Dr. F. Camerel, Dr. R. Ziessel
Ecole Chimie, Polymères, Matériaux (ECPM)
ULP-CNRS (UMR 7509), 25 rue Becquerel
67008 Strasbourg Cedex (France)
E-mail: ziessel@chimie.u-strasbg.fr

[c] B. Paik
Metalurgy and Material Sciences Department
University of Birmingham, Edgbaston
Birmingham B15 2TT (UK)

[d] Dr. M. Schmutz
Institut Charles Sadron, CNRS-UPR 22
6 rue Boussingault, 67083 Strasbourg Cedex (France)

Supporting information for this article is available on the WWW under <http://www.chemeurj.org/> or from the author. It contains additional views of all reported crystal structures, table of solvent screening, additional TEM, powder X-ray diffraction data and the structures of selected nicotinic acid analogues and dyes. Colour versions of Figures 1 to 3 and 6 are also provided.

emerged to afford gels in which the metal plays a central role. For classical organo-gelators, large objects (e.g., fibres, ribbons, layers, etc.) are formed by cooling a hot solution that contains the isolated molecules and are responsible for the gelation of the solvent. In some rare cases, direct dispersion of preassembled large and anisotropic objects from small molecular weight organic molecules can also provide robust gels.^[23] Herein, we present a new organogelator based on an admixture of a nicotinic acid derivative and its sodium salt that together form an extended tube-like one-dimensional structure in the solid state and which is then able to induce gelation of organic solvents.

Results and Discussion

Synthesis: Gelator **7** was prepared by oxidation of methyl-6-methylnicotinate **1** with iodine in DMSO to give the corresponding aldehyde **2** (Scheme 1). Reaction of the aldehyde with trimethylorthoformate in acidic conditions afforded acetal **3**, which was then converted into sodium salt **4** by saponification. Finally treatment with aqueous hydrochloric acid (pH 4) afforded mixture **5**, which contained both the remaining sodium salt and the acid form as the major product. Complete acidification could not be achieved owing to the deprotection of the aldehyde below pH 4.

From mixture **5**, acid form **6** could be isolated as pure crystals, whereas removing the solvent from the remaining aqueous solution yielded gelator **7** as a 1:1 mixture of the acid and the sodium salt (confirmed by elemental analysis). Co-crystallization of acid **6** and its sodium salt **4**, which led to the formation of **7**, in THF afforded single crystals that

were suitable for X-ray diffraction and enabled us to further confirm the stoichiometry (see below). The novelty of these compounds, and presumably the reason why they have not been previously reported, lies in the presence of the orthogonal acid functionality on one end of the molecule and the acetal functionality on the other end. The discovery of the gelation properties was serendipitous; we were preparing these compounds for application in helicate design. However, the observation that **7** exhibited gelation properties, but its component parts **4** or **6** did not, led us to examine the molecular-level interactions in more detail to try to rationalize this observation.

X-ray crystal structure of 6: Acid form **6** was crystallized from the aqueous mother liquor that contained mixture **5**. Rectangular single crystals proved to be suitable for X-ray diffraction and allowed us to resolve the molecular structure of **6**. The molecular structure (Figure 1) consists of infinite

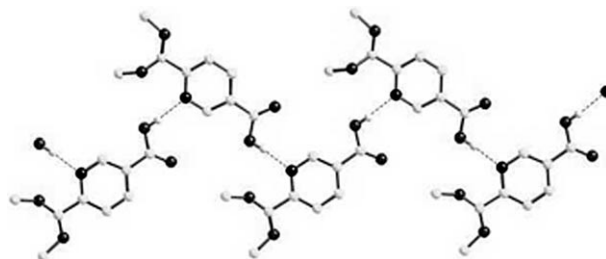
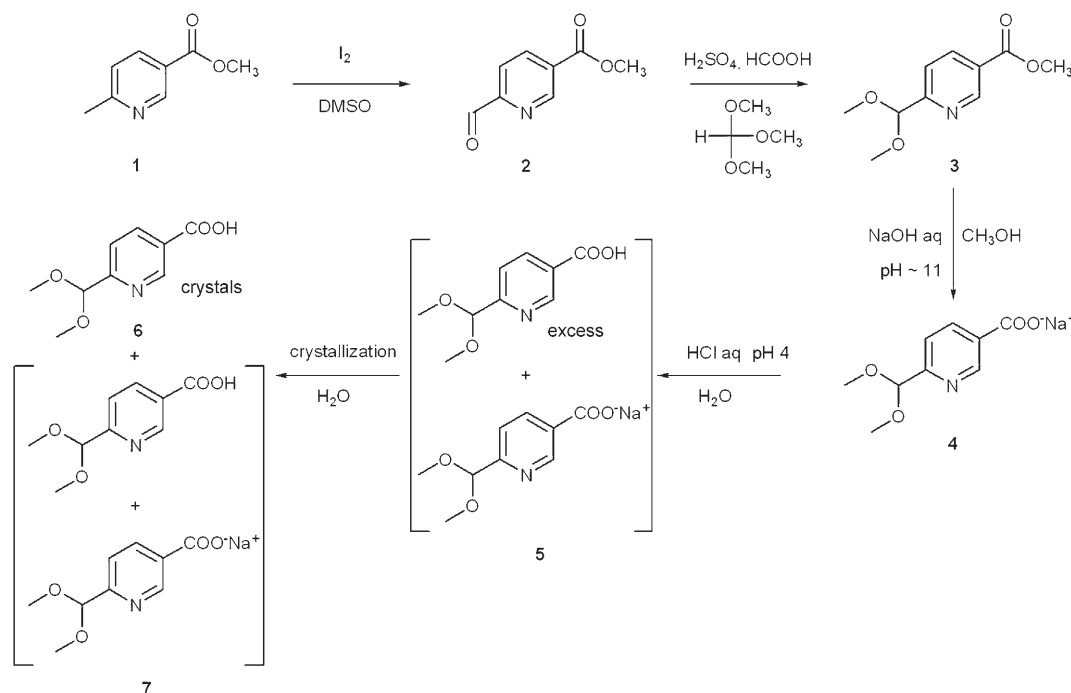


Figure 1. Molecular structure of **6**, which illustrates the assembly into one-dimensional strands through a pyridine-carboxylic acid recognition motif (1.865 and 2.527 Å). Hydrogen atoms, except for those engaged in hydrogen bonding, are omitted for clarity. A colour version of this figure is available in the Supporting Information.



Scheme 1. Synthesis of acid **6** and gelator **7**.

zigzag strands of the nicotinic molecules assembled by hydrogen bonding between the pyridine nitrogen atom and the carboxylic acid hydrogen atom ($\text{O}-\text{H}\cdots\text{N}=1.87 \text{ \AA}$, $\text{O}\cdots\text{N}=2.68 \text{ \AA}$, $\angle\text{O}-\text{H}\cdots\text{N}=170^\circ$). This kind of interaction is well documented in the literature with examples that range from nanotube formation,^[24] molecular complex crystals,^[25] to molecular recognition of a Ce^{IV} -bis(porphyrinate) double decker by diacids^[26] and to the control of organogelation processes.^[18a,27] In addition to this classical hydrogen bond, the other oxygen atom of the acid group (formally the carbonyl oxygen) makes a short contact to H6 of the pyridine ring ($\text{C}-\text{H}\cdots\text{O}=2.53 \text{ \AA}$, $\text{C}\cdots\text{O}=3.26 \text{ \AA}$; Figure S1 in the Supporting Information). Such $\text{C}-\text{H}\cdots\text{O}$ interactions^[28,29] have been observed in other examples of pyridine-carboxylic acid structures and are proposed to afford additional stability and rigidity to the motif.^[30] These one-dimensional strands are then assembled into layers by short interstrand $\text{C}-\text{H}\cdots\text{O}$ and $\pi-\pi$ contacts (Figure S2 in the Supporting Information).

X-ray crystal structure of 7: Single crystals of **7** were isolated from THF and revealed to be a stoichiometric 1:1 mixture of **6** and **4**. The X-ray crystal structure reveals a coordination polymer that contains tube-like chains in which the organic molecules (acid and carboxylate) wrap around the sodium centres (Figure 2).

Within the structure, each molecule of **6** is paired through a hydrogen bond to its carboxylate analogue **4** ($\text{O}-\text{H}\cdots\text{O}=1.65$ and 1.71 \AA , $\angle\text{OHO}=165$ and 161°). In this way two pyridine-acetal units are brought together through a hydrogen bond to effectively create an extended ditopic ligand.^[31,32] There are two distinct types of sodium centre, both of which are five coordinate with approximately square-based pyramidal coordination geometries. The first sodium atom ($\text{Na}_{(1)}$) is bound to a bidentate pyridine-acetal (N,O), a monodentate pyridine and to a bidentate (O,O) binding site created from the carbonyl oxygen atoms at the site in which a hydrogen bond links the acid and carboxylate molecules (see Figure 2 and the Supporting Information). The second sodium atom ($\text{Na}_{(2)}$) is also bound to a bidentate pyridine-acetal (N,O), and to a bidentate (O,O) binding site created from the carbonyl oxygen atoms at the site in which a hydrogen bond links the acid and carboxylate molecules. In this case the fifth coordination position is occupied not by a pyridine nitrogen atom, but rather by one of the carbonyl oxygen atoms that bridges between two metal centres (see Figure 2 and the Supporting Information). There are two distinct pairs of acid-carboxylate dimers. The first binds one sodium at each end (in the pyridine-acetal binding site) and a third sodium at the binding site created at the hydrogen-bond link. The other binds a sodium only at one pyridine-acetal binding site, but binds two sodium atoms at the binding site created at the hydrogen-bond link (see Figure 2). The creation of a bidentate metal binding site linked by a hydrogen bond is not without precedent (coordination to two oximes, one of which is deprotonated and hydrogen bonded to the other would be a classic example),

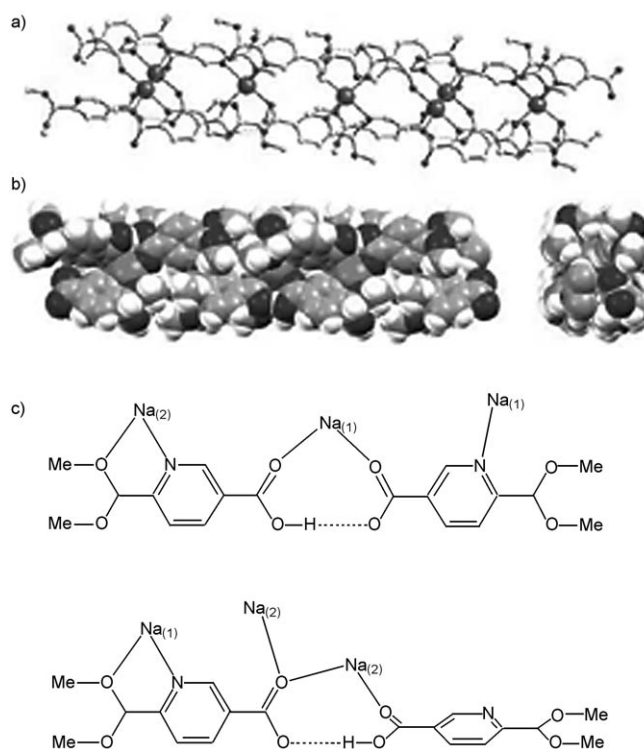


Figure 2. a) A view of **7** that shows how the ligands bind to the two distinct types of five-coordinate sodium centres. Hydrogen atoms (except those involved in hydrogen bonding) are omitted for clarity. b) Two perpendicular space filling views of **7** that illustrate the 1D polymeric strand structure. c) Schematic representation of **7** that shows how the ligand dimers bind to the sodium centres. A colour version, additional views and a schematic illustration of the two coordination environments of $\text{Na}_{(1)}$ and $\text{Na}_{(2)}$ are shown in the Supporting Information.

but the binding of sodium to this particular acid-carboxylate dimer motif does seem to be novel and as can be seen has a dramatic effect in creating a polynucleating ligand that gives rise to a tube-shaped 1D coordination polymer. As will be discussed, the creation of these polymeric tube-like structures seems to be the key feature as to why **7** exhibits gelation properties, whereas its component parts **4** or **6** do not.

Gelation studies: Compound **7** displays gelation properties in a variety of organic solvents that range from polar, non-polar, protic or non-protic to nitrogen containing (Table S1 in the Supporting Information). Gelation tests were performed by sonicating **7** (5 mg) in the considered solvent (250 μL) at temperatures between 37 and 47 $^\circ\text{C}$ for two minutes. Gel formation generally occurred over the minute timescale and was confirmed by simply inverting the vial and observing whether or not the sample flowed. The observed gels (Figure 3) are robust, opaque and display thermoreversible gelation properties. Furthermore, these gels are stable for months and can be loaded with a variety of neutral or zwitterionic dyes (see below).

The ease of the gelation procedure allowed us to investigate a wide range of solvents. Compound **7** was found to have good solubility in water and diols (no gel formation),

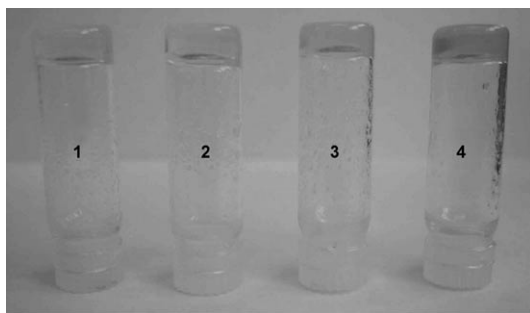


Figure 3. Gelation tests with **7** (5 mg in 250 μL) in 4-methylpyridine (1), 4-methoxypyridine (2), 4-*tert*-butylpyridine (3), and 3-methoxypyridine (4). A colour version of this figure is available in the Supporting Information.

but to be partially soluble in 2-propanol, 2-methyl-1-propanol and 2-ethyl-1-butanol, in which gel formation was observed. Acetone could be gelified as could chlorinated solvents, such as CH_2Cl_2 or 1,2-dichloroethane, but not chloroform. Interestingly, CH_2Cl_2 could be gelified at room temperature in a timescale of minutes without sonication or heating. The minimum gelation concentration was found to be around 10 gL^{-1} in CH_2Cl_2 . This room temperature gelation of CH_2Cl_2 is of particular interest for industrial applications owing to the absence of a heating–dissolution cycle.^[33] Additionally, acetonitrile, pyridine derivatives and some nitrogen-containing bases were also found to gel in the presence of **7** (see Table S1 in the Supporting Information). These gels can also be formed by heating a mixture of **7** and the selected solvent to form a homogeneous fluid solution and then cooling to room temperature. The thermal sol–gel transitions are reversible and were repeated at least four times in CH_2Cl_2 and pyridine without a noticeable sign of weakness in the gel formed. Increasing the temperature above the sol–gel transition temperature leads to the destruction of the interactions that maintain the gel and the mixture then becomes fluid and starts to flow. Visual and microscopic observations performed on the pyridine gel obtained with **7** (25 gL^{-1}) revealed that this gel can resist high temperatures and that the sol–gel phase transition temperature is around 135°C (20°C above the solvent boiling point).^[34] To more accurately quantify the sol–gel transition temperature, differential scanning calorimetry (DSC) experiments and temperature-dependent optical microscopy observations were performed on two gels of **7** in CH_2Cl_2 and in pyridine (25 gL^{-1}). For DSC measurements, the gels were introduced in sealed aluminium pans and scanned in the temperature range of 25 to 150°C (pyridine gel) and 25 to 80°C (CH_2Cl_2 gel). DSC traces of the pyridine gel had one single thermal transition centred at 133.7°C ($\Delta H = 0.085 \text{ J g}^{-1}$) on the first heating curve (Figure S7 in the Supporting Information), which is in good agreement with visual observations. Owing to the low enthalpies involved and the slow nature of gel reformation, no reverse peak could be detected on the DSC cooling curves. The same observations were performed on the CH_2Cl_2 gel with a sol–gel

transition temperature of around 55°C , as evaluated by optical microscopy. A more accurate value of this transition temperature could not be established by DSC, despite several measurements.

TEM, freeze fracture electron microscopy (FFEM) and powder X-ray diffraction (PXRD) studies: TEM experiments were performed to examine the morphology of these gel materials and the nature of the objects that induce gelation. To directly examine the morphology of these objects in the gel state, FFEM experiments were performed on CH_2Cl_2 gels ($c = 16 \text{ gL}^{-1}$). In the gel, a clear lamellar structure is observed that is composed of extended layers (several micrometers) of less than 10 nm in thickness (Figure 4a). The or-

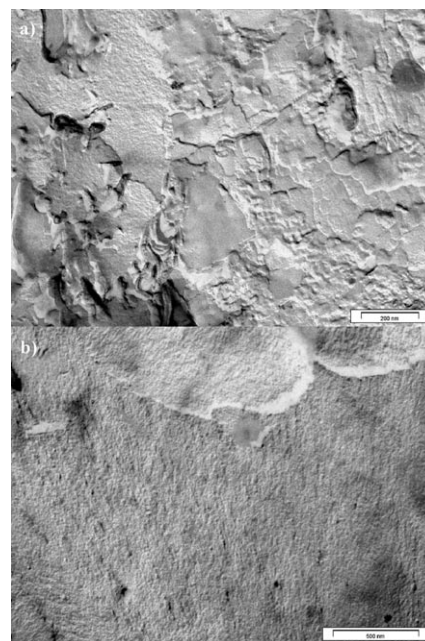


Figure 4. a) Lamellar structure as observed by FFEM of a CH_2Cl_2 gel obtained with **7** ($c = 16 \text{ gL}^{-1}$, scale bar = 200 nm). b) The observed layers display fine striations that correspond to individual fibres in a highly compacted state (periodicity = $5\text{--}6 \text{ nm}$, scale bar = 500 nm).

ganic layers regularly stack to form randomly oriented large lamellar domains. Inside the layers, fine striations are seen that correspond to individual straight chains in a highly compacted state. These fibres are self-assembled into layers with a regular distance ($5\text{--}6 \text{ nm}$, Figure 4b). It appears that the compound is not a classical organogelator in which the formation of a 3D network of entangled fibre-like aggregates is responsible for the immobilization of the solvent.^[1] These microscopic observations reveal that gel formation arises from the self-assembly of lamella composed of fibres in solution.

TEM images obtained from pyridine ($c = 25 \text{ gL}^{-1}$) and CH_2Cl_2 ($c = 16 \text{ gL}^{-1}$) gels dried onto a carbon coated grid reveal the presence of polycrystalline domains (Figure 5a) that is further supported by the electron diffraction pattern

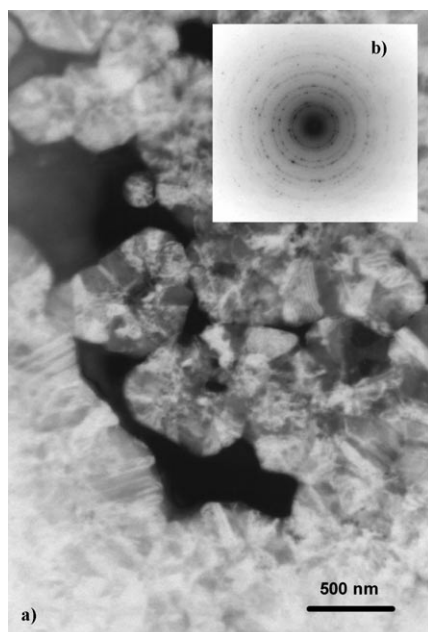


Figure 5. TEM micrographs of a sample of dried pyridine gel, which exhibits crystalline microdomains (a) that were also confirmed by the electron diffraction pattern (b).

determined from a surface analysis of $3.078 \times 10^{-11} \text{ m}^2$ (Figure 5b). Comparison of the data extracted from TEM and the theoretical diffractogram of the crystal structure showed some matches in the 1.60 to 3.30 Å region (Table S2 in the Supporting Information). To investigate this further, PXRD of pyridine and CH_2Cl_2 xerogels were recorded. Comparison of the corresponding PXRD data with that obtained by theoretical methods (from X-ray crystal structure of **7**) for 2θ values in the range of 12 to 45° (around 2 to 7.3 Å) indicated good agreement despite the fact that the match was not perfect, especially with regards to peak intensity. These observations primarily seem to indicate that there is some reminiscence of the crystalline structure inside the gel, such as the molecular order of the metallo-organic sodium-containing tube-like chains that accounts for facile recrystallization after removal of the solvent. It should also be noted that the formation of a woolly sheet-like solid after freeze-drying is in line with a layered structure inside the gel, as observed by FFEM.

FFEM experiments confirm the presence of large objects. The whole set of data (single-crystal and powder X-ray diffraction, DSC, IR spectroscopy and electron microscopy) suggest that there is some reminiscent features of the crystalline 1D architecture in the gel phase. Compound **7** is not a classical organogelator that involves solubilisation/self-assembly processes, but the emergent gel is likely to be formed from a one-dimensional swelling of the crystalline phase.^[35] The intrachain repeat distance, which was extracted from the crystalline structure is one nanometer. The periodicity (5–6 nm) observed inside the layer implies that swelling also occurs inside the layer of chains. The formation of a lamellar phase implies that the swelling is not isotropic,

but principally occurs in one dimension. However, the gels appear to be isotropic when observed by optical microscopy between crossed polarizers, which indicates that they do not form lyotropic liquid crystals in the concentration range explored.

Gel doping: The cohesion/compactness of the gels was qualitatively investigated by diffusion experiments of suitable dyes (related to their solubility) into preformed gels of various solvents. These preliminary experiments showed that gels (e.g., from 2-propanol, acetonitrile, CH_2Cl_2) could be loaded with xylene cyanol FF (XCFF) dye to give blue gels and that the rate of diffusion was dependent on the gel: a solution of XCFF (1.1 mg) in isopropanol (250 μL) deposited on top of a preformed isopropanol gel (4 mg in 250 μL) showed a slow diffusion of the dye into the gel matrix (no diffusion after 1 h; ca. half diffusion after 7 h) compared with the corresponding experiment with a CH_2Cl_2 gel (ca. half diffusion after a few minutes and complete diffusion after 7 h). To further investigate this observation, diffusion experiments of selected dyes into four gel matrices were performed (Figure 6; see Figure S8 in the Supporting Information for the structures of the dyes). The results again revealed differences in gel penetration depending on the solvent that was gelified. The four selected gels were prepared according to the general procedure (**7** (5 mg) in solvent (250 μL)) and a saturated dye solution (250 μL) was deposited on top of the gel.

Dye diffusion was found to be particularly rapid in the CH_2Cl_2 and pyridine gels; complete coloration is observed after only 15 min without destruction of the gels. Diffusion of a solution of phenol red in acetone into a preformed acetone gel resulted in it being almost entirely yellow after 4 h. About 7 h were necessary to observe complete coloration of the 2-propanol gel by the saturated solution of bromothymol blue (BTB) in 2-propanol. These diffusion differences are likely to be related to gel cohesion and the solvent viscosity and mobility inside the gels. It is noteworthy that the additional coloured solution deposited on the top of the gel was completely gelified after some days as long as the minimum gelation concentration was respected.

Features of the structure of **7 required for gelation:** Each of the structural features of the molecule seem to be crucial for gelation (pyridine, carboxylic acid, sodium salt and acetal). For example, the incorporation of cobalt(II) bromide together with gelator **7** in acetonitrile prevented gel formation (cobalt is expected to compete effectively with sodium for pyridine complexation). A variety of molecules based on **7** that did not contain an acetal group failed to give gels (Figure S9 in the Supporting Information). Addition of small amounts (typically 5 μL) of polar solvents (water, ethanol or triethylamine) to a preformed CH_2Cl_2 gel (**7** (5 mg) in solvent (250 μL)) caused instantaneous destruction of the gel. This destruction presumably reflects disruption of hydrogen bonds and metal–ligand coordination and indicates their importance in the gelation process. Sodium

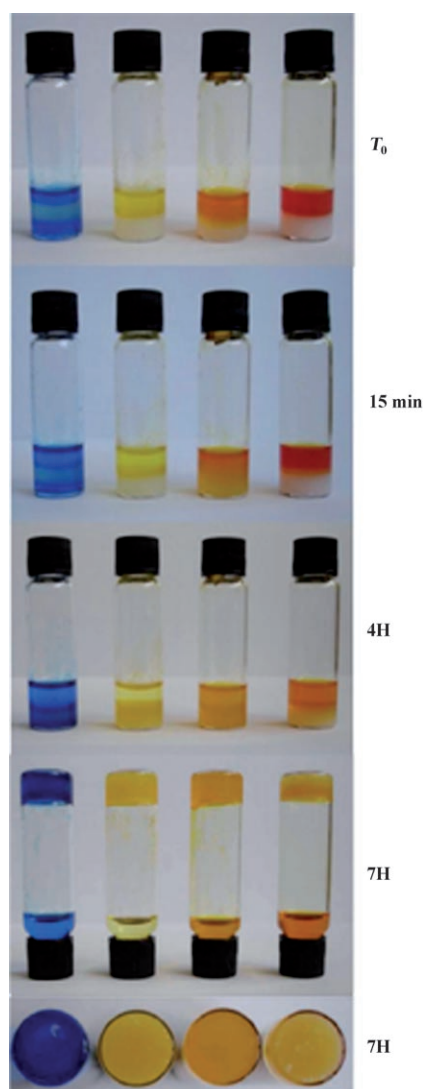


Figure 6. Diffusion of saturated dye solutions into previously prepared gels. (from left to right: solution of XCF in pyridine gel, solution of phenol red in acetone gel, methyl yellow in CH_2Cl_2 gel and BTB in 2-propanol gel).

salt **4** does display some gelation in CH_2Cl_2 and acetonitrile, but kinetically this is a very slow process (at least one week for half of the solvent to become gelled instead of a few minutes after sonication for **7**) and **6** is inactive. The very long time course implied that this gelation ability could merely reflect a slow formation of **7**, or another species. We note that Fages, Vögtle and co-workers have reported that the sodium salts of certain substituted 2,6-pyridinedicarboxylic acids can give rise to gels, although their report was limited to aqueous dimethylsulfoxide.^[36] Noteworthy are also the gelators based on organic salts that consist of imidazolium, dicyclohexyl or dibenzyl ammonium derivatives associated with cinnamate or benzoate counteranions,^[13a,b] as well as those formed from lithocholate sodium salts.^[37] To date, no data related to sodium carboxylate dimers have been reported. Interestingly, the introduction of **6** and its sodium salt **4**

in pyridine or CH_2Cl_2 in a stoichiometry amount did not lead to the formation of a gel after sonication and/or heating. This result implies that the preorganised crystalline structure that provides sodium chains formed through sodium coordination and hydrogen bonding between the carboxylate and acid moieties in compound **7** is mandatory for gel formation.

Conclusion

A new metallo-organic gelator based on an admixture of a nicotinic acid derivative and its sodium salt is reported. The gelator exhibits a large spectrum of activities from spontaneous gelation in CH_2Cl_2 to gelation of more basic solvent like pyridine that exhibits a high thermal resistance. In the solid state, the molecular structure of the gelator is a metallo-organic coordination polymer that contains 1D tubes. In the presence of solvent it appears that the chains may move apart, which allows swelling of the structure and induces the immobilization of the solvent. FFEM clearly demonstrates a lamellar structure that is composed of regular fibres aligned in the lamella. This gelator is a new type of metallo-organic gelator that requires the following conditions: 1) sodium cations, 2) a mixture of the acid and carboxylate in equal parts, 3) the need to preform first the coordination polymer, and 4) weak intermolecular van der Waals type interactions between the coordination polymers that allow the structure to swell to induce the gelification of the solvents. Such sodium driven organisation of hydrogen-bonded organic frameworks is quite remarkable in the sense that it governs not only the growth of the chains, but also indirectly the gelation of the solvents. Doping these gels with strongly absorbing dyes (blue to orange) without breaking the texture of the gels was demonstrated. Clearly, this new gelator could be used as a new template for the production of new one-dimensional objects. Further investigations of the acetal nicotinic acid skeleton are in progress and devoted to form gels by using other molecular structuring units and cations.

Experimental Section

General: All reactants and dyes were purchased from Aldrich and used without further purification. Methyl 6-formylnicotinate **2** was purified by flash chromatography on silica gel 60 (0.040–0.063 mm). ^1H and ^{13}C NMR spectra were recorded at 300 MHz and 75 MHz, respectively, by using Bruker AV and AC 300 spectrometers at 300 K with standard Bruker software. FTIR spectra were recorded by using a Perkin–Elmer SpectrumOne spectrometer as thin films deposited onto dry KBr pellets. DSC was performed by using a Netzsch DSC 200 PC/1 m/H Phox instrument equipped with an intracooler, which allowed measurements from -65 up to 450°C to be recorded. The samples were examined at a scanning rate of 10 K min^{-1} by applying two heating and one cooling cycles. The apparatus was calibrated with indium (156.6°C). Phase behaviour was studied by polarized light optical microscopy (POM) on a Leica DMLB microscope with a Linkam LTS350 hot stage and a Linkam TMS94 central processor. Electrospray ionisation (ESI) analyses were performed at the University of Birmingham by using a Micromass LCT time-of-flight mass spectrometer in positive ionisation mode. Microanaly-

ses were conducted by using a Leeman Labs CE44 CHN analyser at the University of Birmingham.

Methyl 6-formylnicotinate (2): Ester **1** (13 g, 86 mmol) and iodine (8.55 g, 33.7 mmol) were weighed separately and dissolved in the minimum amount of DMSO (around 20 mL) before they were mixed together and added dropwise to DMSO (80 mL) heated to 130 °C. The temperature of the mixture was then slowly raised to 150 °C followed by stirring at this temperature for 30 min. After cooling the solution, the reaction mixture was neutralized with a saturated aqueous solution of Na₂CO₃. The product was extracted with diethyl ether (6 × 150 mL). Evaporation of the solvent gave the crude product, which was purified by two successive column chromatographies (CH₂Cl₂). The product was obtained as an off-white solid (3.41 g, 24%). ¹H NMR (300 MHz, CDCl₃, 298 K): δ = 10.15 (s, 1H; CHO), 9.37 (dd, *J* = 1.8, 0.7 Hz, 1H; Ar-H), 8.48 (ddd, *J* = 8.1, 1.9, 0.9 Hz, 1H; Ar-H), 8.04 (dd, *J* = 8.1, 0.7 Hz, 1H; Ar-H), 4.01 ppm (s, 3H; OCH₃); ¹³C NMR (75 MHz, CDCl₃, 298 K): δ = 192.6, 164.8, 154.9, 151.2, 138.3, 129.2, 121.1, 52.9 ppm; IR (KBr): $\tilde{\nu}$ = 3414 (w), 3065 (w), 2962 (w), 2881 (w), 1717 (s, C=O stretch), 1677 (w), 1592 (m), 1479 (w), 1440 (s), 1389 (s), 1354 (m), 1300 (s), 1285 (s), 1267 (m), 1214 (w), 1193 (m), 1124 (m), 1112 (s), 1020 (s), 945 (m), 879 (w), 855 (m), 813 (m), 769 (m), 694 (m), 634 (m), 483 (w), 412 cm⁻¹ (w); ESI MS (+ve): *m/z*: 166.0 [M+H]⁺; HRMS (EI): *m/z*: calcd: 165.0426 [M]⁺; found: 165.0433 [M]⁺.

Methyl 6-dimethoxymethylnicotinate (3): Ester **2** (0.55 g, 3.33 mmol) was dissolved in trimethylorthoformate (13 mL) and formic acid (1.3 mL) and sulfuric acid (2 drops) were added. The mixture was heated to 50 °C and stirred at this temperature for 10 min, followed by stirring overnight at room temperature. Water (20 mL) and diethyl ether (20 mL) were then added and the aqueous layer was extracted with diethyl ether (2 × 20 mL). The combined organic extracts were washed with saturated aqueous Na₂CO₃ and dried with MgSO₄. Evaporation of the solvent under reduced pressure gave **3** as a yellow oil that turned into an orange–yellow solid at 4 °C (0.62 g, 88%). ¹H NMR (300 MHz, CDCl₃, 298 K): δ = 9.21 (d, *J* = 2.2 Hz, 1H; Ar-H), 8.34 (dd, *J* = 8.1, 2.2 Hz, 1H; Ar-H), 7.65 (d, *J* = 8.1 Hz, 1H; Ar-H), 5.41 (s, 1H; CH), 3.96 (s, 3H; OCH₃), 3.41 ppm (s, 6H; OCH₃); ¹³C NMR (75 MHz, CDCl₃, 298 K): δ = 165.4, 161.0, 150.2, 137.7, 125.7, 120.9, 103.3, 53.6, 52.3 ppm; IR (KBr): $\tilde{\nu}$ = 2956 (w, br), 2835 (w), 1729 (s, C=O stretch), 1600 (m), 1434 (m), 1382 (m), 1352 (m), 1285 (s), 1193 (m), 1109 (s), 1048 (s), 1025 (s), 989 (m), 964 (m), 911 (m), 850 (w), 825 (w), 770 (m), 739 (m), 703 (w), 634 (w), 525 (w), 483 cm⁻¹ (w); ESI MS (+ve): *m/z*: 234.1 [M+Na]⁺; HRMS (ESI): calcd: 234.0742 [M+Na]⁺; found: 234.0738 [M+Na]⁺; elemental analysis calcd (%) for C₁₀H₁₃NO₄: C 56.87, H 6.12, N 6.63; found: C 56.96, H 6.20, N 6.48.

6-Dimethoxymethylnicotinic acid sodium salt (4): Ester **3** (0.558 g, 2.64 mmol) was dissolved in MeOH (5.28 mL) and NaOH (1 m, 5.28 mL) was added. The resulting mixture was stirred overnight before the solvents were evaporated to give the product as a light yellow solid (0.558 g, 96%; contained around 1 equiv NaOH). ¹H NMR (300 MHz, D₂O, 298 K): δ = 8.88 (s, 1H; Ar-H), 8.24 (td, *J* = 8.1, 2.2 Hz, 1H; Ar-H), 7.56 (d, *J* = 8.1 Hz, 1H; Ar-H), 5.44 (s, 1H; CH), 3.41 ppm (m, 6H; OCH₃); ¹³C NMR (75 MHz, D₂O, 298 K): δ = 172.2, 156.4, 148.6, 138.1, 132.1, 120.7, 102.8, 53.7 ppm; IR (KBr): $\tilde{\nu}$ = 3408 (m, very br), 2942 (m, br), 2833 (m), 1603 (s, broad), 1556 (s), 1452 (m, br), 1417 (s), 1370 (m, br), 1286 (w), 1193 (m), 1153 (w), 1106 (s), 1061 (s, br), 1028 (m), 988 (m), 916 (w), 862 (w), 845 (m), 782 (s), 747 (w), 703 (w), 637 (w), 532 (w), 464 cm⁻¹ (w); ESI MS (+ve): *m/z*: 220 [M+H]⁺, 242 [M+Na]⁺; elemental analysis calcd (%) for C₉H₁₀NO₄Na·NaOH: C 41.71, H 4.28, N 5.40; found: C 41.52, H 4.15, N 5.06.

6-Dimethoxymethylnicotinic acid (6): Acid **6** was isolated as crystals from the aqueous mother solution that led to gelator **7** (for the preparation of **7** see below). Crystals of **6** appeared after 3 d at 4 °C from the gelator mother liquor and were collected by filtration and dried overnight (ca. 20 mg). ¹H NMR (300 MHz, D₂O, 298 K): δ = 9.12 (s, 1H; Ar-H), 8.86 (d, *J* = 8.05 Hz, 0.3H; Ar-H), 8.73 (d, *J* = 8.42 Hz, 0.7H; Ar-H), 8.13 (d, *J* = 8.42 Hz, 0.3H; Ar-H), 7.97 (d, *J* = 8.05 Hz, 0.7H; Ar-H), 6.30 (s, 0.3H; CH), 5.74 (s, 0.7H; CH), 3.55 (s, 4.2H; OCH₃), 3.38 ppm (s, 1.6H; OCH₃); ¹³C NMR (75 MHz, D₂O, 298 K): δ = 153.9, 144.6, 141.3, 129.7, 121.7, 99.4, 52.8 ppm; IR (KBr): $\tilde{\nu}$ = 2950 (m), 2914 (m), 2842 (m), 2759

(m, br), 2604 (m, br), 2460 (m, br), 2362 (m), 1896 (w, br), 1713 (s), 1602 (w), 1578 (w), 1450 (w), 1388 (m), 1367 (m), 1354 (m), 1284 (s), 1220 (w), 1202 (w), 1100 (s), 1083 (s), 1032 (m), 982 (w), 962 (m), 902 (w), 852 (w), 808 (w), 763 (s), 727 (w), 683 (w), 652 (m), 566 (w), 523 cm⁻¹ (w); ESI MS (+ve): *m/z*: 197 [M]⁺; elemental analysis calcd (%) for C₉H₁₁NO₄: C 54.82, H 5.62, N 7.10; found: C 55.01, H 5.47, N 7.09.

6-Dimethoxymethylnicotinic acid (6)/6-Dimethoxymethylnicotinic acid sodium salt (4) 1:1 ratio (7): Sodium salt **4** (0.5 g, 2.28 mmol) was dissolved in water prior to acidification with a few drops of aqueous HCl (37%) to pH 4. The solvent was then removed under reduced pressure to a final volume of around 25 mL and left at 4 °C for 3 d. After that time, crystals of the acid appeared and were removed by filtration (see preparation of compound **6**) and the solution was dried under reduced pressure to afford **7** as a yellow powder (475 mg, 95% yield). ¹H NMR (300 MHz, D₂O, 298 K): δ = 8.86 (m, 1H; Ar-H), 8.24 (dd, *J* = 8.1, 1.8 Hz, 1H; Ar-H), 7.55 (d, *J* = 8.1 Hz, 1H; Ar-H), 5.41 (s, 1H; CH), 3.37 ppm (s, 6H; OCH₃); ¹³C NMR (75 MHz, D₂O, 298 K): δ = 170.5, 155.1, 147.2, 137.3, 130.8, 119.7, 101.5, 52.6 ppm; IR (KBr): $\tilde{\nu}$ = 3419 (m, br), 2938 (m, br), 2833 (m), 2359 (w), 1694 (m), 1601 (s), 1556 (s), 1417 (s), 1366 (m), 1286 (w), 1193 (m), 1104 (s), 1059 (s), 1027 (m), 989 (m), 915 (w), 859 (w), 844 (w), 781 (m), 747 (w), 637 (w), 526 (w), 465 cm⁻¹ (w); ESI MS (+ve): *m/z*: 220 [6+Na]⁺, 242 [7+Na]⁺; elemental analysis calcd (%) for C₉H₁₁NO₄·C₉H₁₀NO₄Na: C 51.92, H 5.08, N 6.73; found: C 52.05, H 5.05, N 6.70. Powdered **7** was added to THF and sonicated for 2 min (37–47 °C) for a gelation test in this solvent. A suspension of small crystals was observed and these were used for the X-ray structural determination. It is unclear whether these crystals were formed by or merely revealed by this procedure.

Single-crystal X-ray diffraction: Single-crystal diffraction data were recorded by using a Bruker Smart 6000 diffractometer equipped with a CCD detector and a copper tube source. The structures were solved and refined by using SHELX97^[38] and a riding model was used for the hydrogen atoms during refinement. Crystal data for C₉H₁₁NO₄ (**6**) *M*_r = 197.19; monoclinic; space group *P*2₁/*n*; *a* = 4.073(2), *b* = 11.018(5), *c* = 20.806(9) Å; β = 92.12(3)°, *V* = 933.0(8) Å³; *Z* = 4; ρ_{calcd} = 1.404 g cm⁻³; *F*(000) = 416 μ; Cu_{Kα} = 1.54178 Å; crystal size = 0.25 × 0.20 × 0.20 mm; *T* = 273 (2) K; 4874 reflns collected at 273 K; final *R*₁ = 0.0500 for 1700 reflns with *I* > 2 σ(*I*); *wR*₂ = 0.1306; GOF = 1.006. Crystal data for C₁₈H₂₁N₂O₈ Na (**7**): *M*_r = 416.36; triclinic; space group *P*1; *a* = 11.3701(2), *b* = 11.6587(2), *c* = 16.0520(3) Å; α = 81.5070(10), β = 69.5600(10)°, γ = 87.7460(10); *V* = 1971.85(6) Å³; *Z* = 4; ρ_{calcd} = 1.402 g cm⁻³; *F*(000) = 872 μ; Cu_{Kα} = 1.54178 Å; crystal size = 0.30 × 0.30 × 0.25 mm; *T* = 296 (2) K; 12808 reflns collected at 296 K, final *R*₁ = 0.0554 for 6595 reflns with *I* > 2 σ(*I*), *wR*₂ = 0.1499, GOF = 1.041. CCDC-645324 and -645327 contain the supplementary crystallographic data for this paper. These data can be obtained free of charge from the Cambridge Crystallographic Data Centre via www.ccdc.cam.ac.uk/data_request/cif.

General procedure of gelation experiments: Gelator **7** (5 mg) was added together with the selected solvent (250 μL) in a vial prior to sonication for 2 to 3 min between 37 and 47 °C. The sample was considered to be gelled if the liquid resisted flowing as a result of being turned upside down.

TEM experiments: Pyridine and CH₂Cl₂ gels were prepared according to the general procedure prior to analyses. A tiny amount of sample was directly deposited on a 3.05 mm carbon coated copper grid supplied by Agar Scientific and dried at room temperature. The samples were examined with a Philips CM 20 transmission electron microscope (with LaB₆ filament) operating at 200 kV.

FFEM experiments: FFEM experiments were performed with a CM 12 Philips microscope on metallic replicas of the gels obtained by the freeze fracture technique.

Preparation of samples for PXRD on gels: To avoid possible aggregation owing to the drying process, the CH₂Cl₂ and pyridine gels, which were prepared by dissolving **7** (50 mg) in solvent (2500 μL) and sonicating for 3 min between 37 and 47 °C, were freeze-dried (high vacuum at a temperature below the melting point). In this way, woolly sheet-like solids were obtained and used for PXRD by using a Siemens D5000 diffractometer equipped with a PSD detector and a copper tube source. The samples

were mounted between transparent tapes after grinding and data were recorded at room temperature in transmission mode.

Acknowledgements

This work was supported by the European Union (HPRN-CT-2002-00175; D.B.) and conducted in the context of COST D31 WG D31/0008/04. We thank Lucia Cardo for synthetic assistance and Dr. Dusan Drahnovsky for fruitful discussions.

- [1] a) P. Terech, R. G. Weiss, *Chem. Rev.* **1997**, *97*, 3133–3159; b) L. A. Estroff, A. D. Hamilton, *Chem. Rev.* **2004**, *104*, 1201–1217; c) N. M. Sangeetha, U. Maitra, *Chem. Soc. Rev.* **2005**, *34*, 821–836; d) R. G. Weiss, P. Terech, *Molecular Gels, Materials With Self-Assembled Fibillar Networks*, Springer, Dordrecht, **2006**.
- [2] a) J. J. D. de Jong, L. N. Lucas, R. M. Kellogg, J. H. van Esch, B. L. Feringa, *Science* **2004**, *304*, 278–281; b) S. Yagai, T. Nakajima, K. Kishikawa, S. Kohmoto, T. Karatsu, A. Kitamura, *J. Am. Chem. Soc.* **2005**, *127*, 11134–11139; c) S. Kume, K. Kuroiwa, N. Kimizuka, *Chem. Commun.* **2006**, 2442–2444.
- [3] a) T. Naota, H. J. Koori, *J. Am. Chem. Soc.* **2005**, *127*, 9324–9325; b) J. M. J. Paulusse, R. P. Sijbesma, *Angew. Chem.*, **2006**, *118*, 2392–2396; *Angew. Chem. Int. Ed.* **2006**, *45*, 2334–2337; c) K. Isozaki, H. Takaya, T. Naota, *Angew. Chem.* **2007**, *119*, 2913–2915; *Angew. Chem. Int. Ed.* **2007**, *46*, 2855–2857.
- [4] a) J. B. Beck, S. J. Rowan, *J. Am. Chem. Soc.* **2003**, *125*, 13922–13923; b) S. Wang, W. Shen, Y. Feng, H. Tian, *Chem. Commun.* **2006**, 1497–1499.
- [5] a) R. I. Petrova, J. A. Swift, *J. Am. Chem. Soc.* **2004**, *126*, 1168–1173; b) G. Wulff, B.-O. Chong, U. Kolb, *Angew. Chem.* **2006**, *118*, 3021–3024; *Angew. Chem. Int. Ed.* **2006**, *45*, 2955–2958; c) C. Thiot, M. Schmutz, A. Wagner, C. Mioskowski, *Angew. Chem.* **2006**, *118*, 2934–2937; *Angew. Chem. Int. Ed.* **2006**, *45*, 2868–2871.
- [6] a) K. Sugiyasu, S.-I. Tamaru, M. Takeuchi, D. Berthier, I. Huc, R. Oda, S. Shinkai, *Chem. Commun.* **2002**, 1212–1213; b) K. J. C. van Bommel, A. Friggeri, S. Shinkai, *Angew. Chem.* **2003**, *115*, 1010–1030; *Angew. Chem. Int. Ed.* **2003**, *42*, 980–999, and references therein; c) J. H. Jung, S.-H. Lee, J. S. Yoo, K. Yoshida, T. Shimizu, S. Shinkai, *Chem. Eur. J.* **2003**, *9*, 5307–5313; d) G. Roy, J. F. Miravet, B. Escuder, C. Sanchez, M. Llugar, *J. Mater. Chem.* **2006**, *16*, 1817–1824; e) S. Ray, A. K. Das, A. Banerjee, *Chem. Commun.* **2006**, 2816–2818; f) S. Bhattacharya, A. Srivastava, A. Pal, *Angew. Chem.* **2006**, *118*, 3000–3003; *Angew. Chem. Int. Ed.* **2006**, *45*, 2934–2937.
- [7] a) W. Gu, L. Lu, G. B. Chapman, R. G. Weiss, *Chem. Commun.* **1997**, 543–544; b) R. J. H. Hafkamp, B. P. A. Kokke, I. M. Danke, H. P. M. Geurts, A. E. Rowan, M. C. Feiters, R. J. M. Nolte, *Chem. Commun.* **1997**, 545–546.
- [8] a) A. Ajayaghosh, S. J. George, V. K. Praveen, *Angew. Chem.* **2003**, *115*, 346–349; *Angew. Chem. Int. Ed.* **2003**, *42*, 332–335; b) K. Sugiyasu, N. Fujita, S. Shinkai, *Angew. Chem.* **2004**, *116*, 1249–1253; *Angew. Chem. Int. Ed.* **2004**, *43*, 1229–1233.
- [9] a) Y. Koshi, E. Nakata, H. Yamane, I. Hamachi, *J. Am. Chem. Soc.* **2006**, *128*, 10413–10422; b) P. Mukhopadhyay, Y. Iwashita, M. Shirakawa, S.-I. Kawano, N. Fujita, S. Shinkai, *Angew. Chem.* **2006**, *118*, 1622–1625; *Angew. Chem. Int. Ed.*, **2006**, *45*, 1592–1595; c) S. Bhuniya, B. H. Kim, *Chem. Commun.* **2006**, 1842–1844.
- [10] a) G. A. Silva, C. Czeisler, K. L. Niece, E. Beniash, D. A. Harrington, J. A. Kessler, S. I. Stupp, *Science* **2004**, *303*, 1352–1355; b) S. Nayak, L. A. Lyon, *Angew. Chem.* **2005**, *117*, 7862–7886; *Angew. Chem. Int. Ed.* **2005**, *44*, 7686–7708; c) P. K. Vemula, J. Li, G. John, *J. Am. Chem. Soc.* **2006**, *128*, 8932–8938; d) G. John, G. Zhu, J. Li, J. S. Dordick, *Angew. Chem.*, **2006**, *118*, 4890–4893; *Angew. Chem. Int. Ed.* **2006**, *45*, 4772–4775; e) D. K. Smith, *Chem. Commun.* **2006**, 34–44.
- [11] V. K. Praveen, S. J. George, R. Varghese, C. Vijayakumar, A. Ajayaghosh, *J. Am. Chem. Soc.* **2006**, *128*, 7542–7550.
- [12] a) J.-H. Fuhrhop, W. Helfrich, *Chem. Rev.* **1993**, *93*, 1565–1582; b) D. Pasini, A. Kraft, *Curr. Opinion Solid State Mater. Sci.* **2004**, *8*, 157–163.
- [13] a) A. Ballabh, D. R. Trivedi, P. Dastidar, *Chem. Mater.* **2003**, *15*, 2136–2140; b) D. R. Trivedi, A. Ballabh, P. Dastidar, *Cryst. Growth Des.* **2006**, *6*, 763–768; c) P. Terech, A. de Geyer, B. Struth, Y. Talmon, *Adv. Mater.* **2002**, *14*, 495–498; d) P. Terech, B. Jean, F. Ne, *Adv. Mater.* **2006**, *18*, 1571–1574.
- [14] a) J.-L. Pozzo, G. M. Clavier, J.-P. Desvergne, *J. Mater. Chem.* **1998**, *8*, 2575–2577; b) J. H. van Esch, B. L. Feringa, *Angew. Chem.* **2000**, *112*, 2351–2354; *Angew. Chem. Int. Ed.* **2000**, *39*, 2263–2266; c) R. Luboradzki, O. Gronwald, M. Ikeda, S. Shinkai, D. N. Reinhoudt, *Tetrahedron* **2000**, *56*, 9595–9599; d) S.-I. Tamaru, M. Nakamura, M. Takeuchi, S. Shinkai, *Org. Lett.* **2001**, *3*, 3631–3634; e) H. Kobayashi, A. Friggeri, K. Koumoto, M. Amaike, S. Shinkai, D. N. Reinhoudt, *Org. Lett.* **2002**, *4*, 1423–1426.
- [15] a) S. Shinkai, K. Murata, *J. Mater. Chem.* **1998**, *8*, 485–495; b) T. Ishi-i, R. Iguchi, E. Snip, M. Ikeda, S. Shinkai, *Langmuir* **2001**, *17*, 5825–5833; c) N. M. Sangeetha, S. Bhat, A. R. Choudhury, U. Maitra, P. Terech, *J. Phys. Chem. B* **2004**, *108*, 16056–16063; d) S. Mukhopadhyay, U. Maitra, I. A. G. Krishnamoorthy, J. Schmidt, Y. Talmon, *J. Am. Chem. Soc.* **2004**, *126*, 15905–15914.
- [16] a) G. Mieden-Gundert, L. Klein, M. Fischer, F. Vögtle, K. Heuzé, J.-L. Pozzo, M. Vallier, F. Fages, *Angew. Chem.* **2001**, *113*, 3266–3267; *Angew. Chem. Int. Ed.* **2001**, *40*, 3164–3166; b) V. Caplar, M. Zinic, J.-L. Pozzo, F. Fages, G. Mieden-Gundert, F. Vögtle, *Eur. J. Org. Chem.* **2004**, 4048–4059; c) D. Das, A. Dasgupta, S. Roy, R. N. Mitra, S. Debnath, P. K. Das, *Chem. Eur. J.* **2006**, *12*, 5068–5074; d) Z. Yang, G. Liang, B. Xu, *Chem. Commun.* **2006**, 738–740.
- [17] S.-I. Tamaru, S.-Y. Uchino, M. Takeuchi, M. Ikeda, T. Hatano, S. Shinkai, *Tetrahedron Lett.* **2002**, *43*, 3751–3755.
- [18] a) O. Gronwald, S. Shinkai, *Chem. Eur. J.* **2001**, *7*, 4328–4334; b) A. Friggeri, O. Gronwald, K. J. C. van Bommel, S. Shinkai, D. N. Reinhoudt, *J. Am. Chem. Soc.* **2002**, *124*, 10754–10758; c) R. Luboradzki, Z. Pakulski, *Tetrahedron* **2004**, *60*, 4613–4616; d) R. Luboradzki, Z. Pakulski, B. Sartowska, *Tetrahedron* **2005**, *61*, 10122–10128.
- [19] A. R. Hirst, D. K. Smith, J. P. Harrington, *Chem. Eur. J.* **2005**, *11*, 6552–6559, and references therein.
- [20] a) M. Shirakawa, N. Fujita, S. Shinkai, *J. Am. Chem. Soc.* **2003**, *125*, 9902–9903; b) S.-I. Kawano, S.-I. Tamaru, N. Fujita, S. Shinkai, *Chem. Eur. J.* **2004**, *10*, 343–351.
- [21] a) R. Oda, I. Huc, S. J. Candau, *Angew. Chem.* **1998**, *110*, 2835–2838; *Angew. Chem. Int. Ed.* **1998**, *37*, 2689–2691; b) R. Oda, I. Huc, M. Schmutz, S. J. Candau, F. C. MacKintosh, *Nature* **1999**, *399*, 566–569.
- [22] a) N. Amanokura, Y. Kanekiyo, S. Shinkai, D. N. Reinhoudt, *J. Chem. Soc. Perkin Trans. 2* **1999**, 1995–2000; b) R. Ziessel, G. Pickaert, F. Camerel, B. Donnio, D. Guillon, M. Cesario, T. Prangé, *J. Am. Chem. Soc.* **2004**, *126*, 12403–12413; c) S.-I. Kawano, N. Fujita, S. Shinkai, *J. Am. Chem. Soc.* **2004**, *126*, 8592–8593; d) K. Kuroiwa, T. Shibata, A. Takada, N. Nemoto, N. Kimizuka, *J. Am. Chem. Soc.* **2004**, *126*, 2016–2021; e) A. Kishimura, T. Yamashita, T. Aida, *J. Am. Chem. Soc.* **2005**, *127*, 179–183; f) F. Fages, *Angew. Chem.* **2006**, *118*, 1710–1712; *Angew. Chem. Int. Ed.* **2006**, *45*, 1680–1682; g) P. C. Andrews, P. C. Junk, M. Massi, M. Silberstein, *Chem. Commun.* **2006**, 3317–3319; h) F. Camerel, R. Ziessel, B. Donnio, D. Guillon, *New J. Chem.* **2006**, *30*, 135–139.
- [23] F. Camerel, B. Donnio, C. Bourgoigne, M. Schmutz, D. Guillon, P. Davidson, R. Ziessel, *Chem. Eur. J.* **2006**, *12*, 4261–4274.
- [24] Y. Tian, Q. He, Y. Cui, C. Tao, J. Li, *Chem. Eur. J.* **2006**, *12*, 4808–4812.
- [25] a) C. B. Aakeröy, A. M. Beatty, B. A. Helfrich, *J. Am. Chem. Soc.* **2002**, *124*, 14425–14432; b) S. Varughese, V. R. Pedireddi, *Chem. Eur. J.* **2006**, *12*, 1597–1609.
- [26] M. Takeuchi, T. Imada, S. Shinkai, *Angew. Chem.* **1998**, *110*, 2242–2246; *Angew. Chem. Int. Ed.* **1998**, *37*, 2096–2099.
- [27] S. Tanaka, M. Shirakawa, K. Kaneko, M. Takeuchi, S. Shinkai, *Langmuir* **2005**, *21*, 2163–2172.

- [28] a) R. Taylor, O. Kennard, *J. Am. Chem. Soc.* **1982**, *104*, 5063–5070; b) G. R. Desiraju, *Acc. Chem. Res.* **1991**, *24*, 290–296; c) R. K. Castellano, *Curr. Org. Chem.* **2004**, *8*, 845–865; d) Z.-G. Wang, B.-H. Zhou, Y.-F. Chen, G.-D. Yin, Y.-T. Li, A.-X. Wu, L. Isaacs, *J. Org. Chem.* **2006**, *71*, 4502–4508.
- [29] T. Kato, N. Mizoshita, K. Kishimoto, *Angew. Chem.* **2006**, *118*, 44–74; *Angew. Chem. Int. Ed.* **2006**, *45*, 38–68.
- [30] a) F. H. Allen, J. E. Davies, J. J. Galloy, O. Johnson, O. Kennard, C. F. Macrae, D. G. Watson, *J. Chem. Inf. Comput. Sci.* **1991**, *31*, 187–204; b) C. V. K. Sharma, M. J. Zaworotko, *Chem. Commun.* **1996**, 2655–2656.
- [31] As further confirmation that the OH group of the acid fragment is engaged in hydrogen-bonded motifs inside the solid-state structure, infrared spectroscopy was performed on powder sandwiched between anhydrous KBr pellets. The IR spectrum displays a group of small bands located between 3000 and 2000 cm^{-1} (ν_{OH}) and two other bands located at 1394 and 1287 cm^{-1} (for in-plane O–H bending and C–O stretching vibrations), which is characteristic of OH groups engaged in hydrogen bonding. The ν_{OH} band at 3350 cm^{-1} , characteristic of a free acid function, was not detected.
- [32] K. Nakanishi, *Infrared Absorption Spectroscopy*, Holden-Day, **1962**.
- [33] M. Suzuki, Y. Nakajima, M. Yumoto, M. Kimura, H. Shirai, K. Hanabusa, *Langmuir* **2003**, *19*, 8622–8624.
- [34] J. Makarevic, M. Jokic, L. Frkanec, D. Katalenic, M. Zinic, *Chem. Commun.* **2002**, 2238–2239.
- [35] a) J. Sayettat, L. M. Bull, J.-C. P. Gabriel, S. Jobic, F. Camerel, A.-M. Marie, M. Fourmigué, P. Batail, R. Brec, R.-L. Inglebert, *Angew. Chem.* **1998**, *110*, 1773–1776; *Angew. Chem. Int. Ed.* **1998**, *37*, 1711–1714; b) J. C. P. Gabriel, F. Camerel, P. Batail, P. Davidson, B. Lemaire, H. Desvaux, *Nature* **2001**, *413*, 504–508.
- [36] W. M. Müller, U. Müller, G. Mieden-Gundert, F. Vögtle, M. Lescanne, K. Heuzé, A. D'Aléo, F. Fages, *Eur. J. Org. Chem.* **2002**, 2891–2893.
- [37] a) P. Terech, W. G. Smith, R. G. Weiss, *J. Chem. Soc. Faraday Trans.* **1996**, *92*, 3157–3162; b) P. Terech, N. M. Sangeetha, S. Bhat, J.-J. Al-legraud, E. Buhler, *Soft Matter* **2006**, *2*, 517–522.
- [38] G. M. Sheldrick, SHELX97 (Includes SHELXS97, SHELXL97), Programs for Crystal Structure Analysis, Institut für Anorganische Chemie der Universität Göttingen, Göttingen, Germany, **1998**.

Received: May 2, 2007
Published online: September 11, 2007